行政院國家科學委員會專題研究計畫 成果報告

龍葵萃取物防、抗肝癌能力分子作用機轉之探討
研究成果報告(精簡版)

計 畫 類 別 ：個別型
計 畫 編 號 ：NSC 95-2320-B-040-022-
執 行 期 間 ：95 年 08 月 01 日至 96 年 07 月 31 日
執 行 單 位 ：中山醫學大學生化暨生物科技研究所

計畫主持人：周芬碧

計畫參與人員：博士生：林惠美、彭佩玲

處 理 方 式 ：本計畫涉及專利或其他智慧財產權，1 年後可公開查詢

中 華 民 國 96 年 10 月 29 日

附件一

行政院國家科學委員會補助專題研究計畫 ■ 成 果 報 告 □期中進度報告

龍葵萃取物防、抗肝癌能力分子作用機轉之探討

計畫類別：■ 個別型計畫　　□ 整合型計畫
計畫編號：NSC 95－2320－B－040－022－
執行期間：　95 年 08 月 01 日至　96 年 07 月 31 日

計畫主持人：周芬碧
共同主持人：
計畫參與人員：博士生 林惠美
　　　　　　　博士生 彭佩玲

成果報告類型(依經費核定清單規定繳交)：■精簡報告　□完整報告

本成果報告包括以下應繳交之附件：
□赴國外出差或研習心得報告一份
□赴大陸地區出差或研習心得報告一份
□出席國際學術會議心得報告及發表之論文各一份
□國際合作研究計畫國外研究報告書一份

處理方式：除產學合作研究計畫、提升產業技術及人才培育研究計畫、列管計畫及下列情形者外，得立即公開查詢
　　□涉及專利或其他智慧財產權，■一年□二年後可公開查詢

執行單位：中山醫學大學生化暨生物科技研究所

中　華　民　國　　96 年　　10 月　　15 日

中文摘要

關鍵詞：龍葵；細胞凋亡；自體吞噬；抗腫瘤活性

在中醫學的領域裡，龍葵是一種被廣泛用來治療癌症的中草藥植物，對肝癌、乳癌、肺癌、胃癌、大腸癌及膀胱癌等均具有顯著療效，亦有報導指出，其具有保肝、抗發炎的效果，然而龍葵保肝及抗肝癌之能力、有效活性成分及作用機轉，並無確切可引用的報告。本計畫擬以萃取龍葵萃取物(SNE)處理肝癌細胞，探討其抗肝癌之能力及詳細之分子機轉。結果顯示，SNE 對肝癌細胞之毒性顯著大於正常肝細胞，高濃度 SNE 處理之下，可活化細胞內 p-JNK, Bax, cytochrome *c*, 及 cleaved-caspase 3 之表現，使肝癌細胞透過 apoptosis 機制走向凋亡，低濃度之 SNE 處理，則可活化細胞內 autophagic protein 之表現，促進肝癌細胞透過 autophagy 機轉死亡。此研究結果為肝癌之防治及治療提供了一個新的方向。

英文摘要

Key words: *Solanum Nigrum* Linn; apoptosis; autophagy; acidic vesicular organelle; antineoplastic activity

Solanum nigrum L. (SN) has been used in traditional folk medicine to treat different cancers. It is also used as a hepatoprotective and anti-inflammatory agent. In this study, we demonstrated that the extract of SN (SNE) induced a strong cytotoxic effect toward HepG2 cells but much less to Chang liver and WRL-68 cells. The mechanisms of the cytotoxic effect were concentration-dependent. High doses of SNE (2 and 5 mg/mL) induced apoptotic cell death in HepG2 cells, as evidenced by increases in the expressions of p-JNK and Bax, mitochodrial release of cytochrome c, and caspase activation. On the other hand, cells treated with low concentrations of SNE (50-1000 μg/mL) revealed morphological and ultrastructural changes of autophagocytic death under electron microscopic observation. Furthermore, these cells showed increased levels of autophagic vacuoles and LC3-I and LC3-II proteins, specific markers of autophagy. The levels of Bcl-2 and Akt that have been implicated in the down-regulation of autophagy were decreased upon SNE treatment. Taken together, these findings indicate that SNE induced cell death in hepatoma cells via two distinct antineoplastic activities of SNE, the ability to induce apoptosis and autophagocytosis, therefore suggesting that it may provide leverage to treat liver cancer.

INTRODUCTION

Hepatocellular carcinoma (HCC) is a deadly disease with poor prognosis and a 5-year survival rate of about 5%. It is one of the most common human malignancies in sub-Saharan Africa, South East Asia and China. (*1*). According to the World Health Organization statistics, of 6,350,000 cancer cases reported each year, 4% are hepatocellular carcinoma, 42% of which occur in China. Traditional treatment of liver tumors typically has been surgical resection and chemotherapeutics. However, these commonly used techniques are frequently challenged in view of metastasis and other pathological changes. Therefore, the development of new agents for hepatocellular cancer is important to reduce the mortality caused by this disease.

Solanum nigrum L. (SN) is a herbal plant indigenous to Asia, and grows wildly and abundantly in open fields. It has been used in traditional Oriental medicines for treating a various kinds of tumors and is believed to have various biological activities (*2*). Previous investigations have shown that extracts of SN suppressed the oxidant mediated DNA-sugar damage (*3*), and the plant exerted cytoprotection against gentamicin-induced toxicity on Vero cells (*4*) and anti-neoplastic activity against Sarcoma 180 in mice (*5*). More recent studies revealed that extracts of SN induced apoptosis in MCF-7 cells (*2*) and inhibited 12-O-tetradecanoylphorbol 13-acetate (TPA)-induced tumor promotion in HCT-116 cells (*6*). These studies suggest that SN possesses a beneficial activity as anti-oxidant and anti-tumor promoting agent, although the mechanism for the activity remains to be elucidated.

In Chinese traditional medicine, SN is believed to have anti-tumor properties, including liver cancer, breast cancer, lung cancer, stomach cancer, colon cancer and bladder cancer, and is also used as hepatoprotective and anti-inflammation agent, although the mechanism for the activity remains to be elucidated (*3, 4*). The latest report revealed that the ethanol extract of dried fruits of *Solanum nigrum* has a remarkable hepatoprotective effect against the CCl_4-induced liver damage (*7*). This study developed some understanding of the effects of SN on liver cancer cells to evaluate its therapeutic application in treating liver cancer.

SN has been reported to contain many polyphenolic compounds, mainly flavonoids and steroids. The antioxidant and anti-tumor activity of SN may be due to the presence of polyphenolic constituents. The presence of steroidal glycosides, steroidal alkaroids, steroidal oligoglycosides, solamargine, and solasonine has also been detected (*8*).The purpose of this work was to study the effects of SN on liver cancer cells to evaluate its therapeutic potential in treating liver cancer. In this report, we describe experiments that showed water extracts of SN induced programmed cell death in liver cancer cells. The death mechanism was characterized, revealing that SN not only initiated apoptosis but also caused cell death through autophagocytosis (type II programmed cell death). The results of this investigation provide a scientific evidence for the application of this herbal medicine in liver cancer therapy.

MATERIALS AND METHODS

Preparation of Extracts of SN (SNE). The whole plant of SN was collected from the mountain in Miaoli, Taiwan. The plants were washed, cut into small pieces, shade dried for 3 days, and then dried overnight in an oven. The dried SN (800 g) was mix with water (5000 ml) for 30 minutes, and subjected to continuous hot extraction (100℃, 40 minutes). The resulted water extract was filtered and subsequently concentrated with water bath (90℃) until became creamy, and dried in an oven (70℃) that finally gave 185 g (23.125 % of initial amount) of powder (water extract of SN). The concentration used in the experiment was based on the dry weight of the extract.

Determination of Total Phenolics, polysaccharide and protein. The concentration of total phenols was analyzed according to the Folin-Ciocalteu method (*9*). The contents of polysaccharide and protein in SNE were determined using the phenol-sulfuric acid method and Bio-Rad protein assay kit, respectively.

Characterization of phenolic compounds of SNE. Analyses were performed on a Finnigan Surveyor Modular HPLC system (Thermo Electron Co., USA). The chromatographic separation of the compounds was achieved using an analytical column: Luna 3μ C18(2) 150 × 2.0 mm and guard column, SecurityGuard C18 (ODS) 4 × 3.0 mm ID (Phenomenex, Inc., Torrance, CA.) ata flow rate of 0.2 mL/min. Mobile phases A and B were water and acetonitrile, respectively, both containing 0.1% formic acid. Gradient elution was conducted as follows: 0-15 min of 5% B, 15-50 min of 5-40% B and 50-55 min of 40-95% B with a linear gradient, followed by 55-65 min of 95% B isocratic. Photodiode array detector (PDA) was operated at wavelengths between 220 and 400 nm. The system was coupled to a Finnigan LCQ Advantage MAX ion trap mass spectrometer, and operated in electrospray ionization (ESI) mode. Samples of 20 μl of extracts were directly injected into the column using a Rheodyne (model 7725i) injection valve. ESI source and negative ionization mode was used with different fragment voltages. Nitrogen was used as the neutralizing and drying gas. The typical operating parameters were as follows: spray needle voltage, 5 kV; ion transfer capillary temperature, 300 °C; nitrogen sheath gas, 40; and auxiliary gas, 5 (arbitrary units). The ion trap contained helium damping gas which was introduced in accordance with the manufacturer's recommendations. Mass spectra were acquired in a *m/z* range of 100-1000, with 5 microscans and a maximum ion injection time of 200 ms. The SIM analysis was a narrow scan event that monitored the *m/z* value of the selected ion, in a range of 1.0 Th centred on the peak for the molecular ion; this function was used in the analysis of molecular ions of the flavonoids for MS/MS in negative ESI modes. The MS/MS fragment spectra were produced using normalized collision energies with an increment of 30%, and also with wideband activation 'OFF' (*10*).

Determination of Cell Viability (MTT Assay). To evaluate the cytotoxicity of SNE, MTT [3-(4,5-dimethylthiazol-2-yl)-2,5-diphenyltetrazolium bromide] assay was performed to determine the cell viability (*11*). Cells were seeded in 24-well plates at a density of 3.5×10^4 cells/well, and treated with SNE at 0~5 mg/ml concentration at 37℃ for 24 h and 48 h. In inhibition experiments, cells were pre-treated with 2 mM of 3-MA. After the exposure, media were removed, and the cells were washed with PBS. Thereafter, the medium was changed to the one containing 100 μl MTT (5 mg/ml) /well for another 4 h-incubation. The viable cell number per dish is directly proportional to the production of formazan, which was solubilized in isopropanol, and measured spectrophotometrically at 563 nm.

Flow Cytometric Analysis. Cells synchronized at the G_0 phase by serum starvation for 24 h were incubated in fresh medium containing 10% v/v FBS to allow the progression through the cell cycle. At various time periods after relief of the quiescent state, the cells were analyzed for cell cycle distribution by flow cytometry (*12*).

Western Blot Analysis. After the indicated SNE treatment, cell lysate was then subjected to a centrifugation of 10,000 $\times g$ for 10 min at 4℃. Resultant protein samples were separated in a 12.5% polyacrylamide gel, and transferred onto a nitrocellulose membrane as previously described. The blot was sequentially incubated with 5% non-fat milk in PBS for 1 h to block non-specific binding, with a polyclonal antibody against phospho-JNK, phospho-Akt (Cell Signaling Tech. MA, USA), Bax, cytochrome *c*, caspase 3, Bcl-2 (Senta Cruz. CA, USA) or LC3 (kindly provided by Drs Yoshimori and Mizushima, National Institute for Basic Biology, Okazaki, Japan) for 2 h, and then with an appropriate peroxidase-conjugated secondary antibody (Sigma, St. Louis, MO) for 1 h. All incubations were carried out at 37℃, and intensive PBS washing was performed between each incubation. After the final PBS wash, signal was developed by 4-chloro-1-napthol /3,3-o-diaminobenzidine, and relative photographic density was quantitated by scanning the photographic negatives by a gel documentation and analysis system (Alpha Imager 2000, Alpha Innotech Corporation, San Leandro, CA, USA).

Eletron Microscopy. The cells were harvested by trypsinization, washed twice with PBS, and fixed with 2% glutaraldehyde, 4% paraformaldehyde and 1% tannic acid in 0.1 mol/l cacodylate buffer, pH 7.4, for 25 h at 4℃. After washing with PBS, the cells were stained with an osmium-thiocarbohydrazide-osmium (OTO). This procedure was carried out by incubating cells in 1% OsO_4 in 0.1 mol/l cacodylate buffer, pH 7.4, for one hour followed by 1% thiocarbohydrazide in H_2O for 15 minutes and then 1% OsO_4 for 15 minutes. Extensive washing of cells with distilled water was performed between each step. After staining, the cells were dehydrated in a graded series of EtOH to 100% EtOH and then immersed serially with 1:1 hexamethyldisilazane and absolute ethanol, and pure hexamethyldisilazane for five minutes each. After air drying from hexamethyldisilazane for overnight, the cells were embedded in agarose gel. One-μm thin sections were cut and the gels were coated with

500 Å of gold in a JEOL Vacuum sputter coater and viewed in a JEOL T300 electron microscope with scanning attachment (JEOL, Tokyo, Japan) (*13*).

Detection of Acidic Vesicular Organelles (AVO) With Acridine Orange Staining. To detect AVOs in SNE-treated cells, the vital staining with acridine orange was performed as described previously (*14*). The treated-tumor cells were stained with acridine orange, adding at a final concentration of 1 μg/ml for 15 minutes. Samples were then examed under a fluorescence microscope. Acridine orange labels acidic vesicular organelles, such as autophagosomes. A typical acridine orange-positive cell exhibits granular distribution of acridine orange in the cytoplasm indicative of autophagosome formation.

Statistical Analysis. Statistical significances were analyzed by one-way analysis of variance (ANOVA) with *post-hock* Dunnett's test. *p*-value ≦ 0.05 was considered statistically significant (Sigma-Stat 2.0, Jandel Scientific, San Rafael, CA, USA).

RESULTS

Composition of SNE. To establish the composition of SNE from *Solanum Nigrum* L., the contents of polyphenol and polysaccharide were assayed, and the concentrations of polyphenolic acids were determined by HPLC. As show in Table 1, the dry weight yield of SNE was 23.125 ± 2.095%, consisting of 20.35 ± 0.967% total polyphenolics using gallic acid as standard and 14.92 ± 1.333% polysaccharide. Polysaccharide is usually associated with protein as complexes, the result indicated SNE contained 4.81 ± 0.442% of protein. HPLC analysis of the standard polyphenols showed the retention times (RT) of gallic aicd, protocatechuic acid (PCA), catechin, caffeic acid, epicatechin, rutin and naringenin were 6.2, 13.49, 31.48, 32.84, 35.61, 4.035 and 49.16 min, respectively (Figure 1, Table 2). The analysis of SNE revealed the presence of gallic aicd (2.897%), PCA (1.977%), catechin (2.353%), caffeic acid (1.988%), epicatechin (0.392%), rutin (0.836%) and naringenin (5.106%). The further identities of the 7components were established from recorded mass spectra. The mass spectra of the phenolic acids are listed in Table 2. The extract was stored at -20℃ and used in the following studies. In the present study, we have identified the contents of polysaccharides and proteins in SNE and characterized seven phenolic compounds of SNE.

Cytotoxic Effects of SNE on HepG2 Cells. In this study, we first determined the cytotoxicity of SNE by treating HepG2, WRL-68 and Chang liver cells with SNE at various concentrations for 24 h and 48 h followed by MTT assay. The human hepatic cell line WRL-68 has a morphological structure similar to hepatocytes and hepatic primary cultures. Derived from fetal liver, WRL-68 cells secrete α-fetoprotein and albumin, preserve the activity of some characteristic or specific liver enzymes (i.e. alanine aminotransferase, aspartate aminotransferase, γ-glutamyl transpeptidase and alkaline phosphatase) and exhibit a cytokeratin pattern similar to other hepatic cultures, providing an in vitro model to study the toxic effects of xenobiotics (*15*).

The addition of SNE exerted a cytotoxic effect in a dose- and time-dependent manner (Figure 2AB). Following a 24 h incubation with 50 μg/ml of SNE in HepG2 cells, the cytotoxicity was around 22.7~27.4% (Figure 2A). However, when 100~5000 μg/ml of the extract was added, a significant increase in cytotoxicity was observed. Furthermore, a time-dependent increase in SNE-induced cytotoxicity was also detected (Figure 2B). The strongest potency of SNE on the cytotoxicity of cells was toward HepG2 liver cancer cells. The concentration of SNE on the inhibition of 50% of HepG2 cells viability (IC_{50}) was 0.625 mg/ml. However, the IC_{50} of SNE to the death of Chang liver (human liver cells; IC_{50}: 3.2 mg/ml SNE) and WRL-68 (human fetal liver cell; IC_{50}: 3.0 mg/ml SNE) were 5.12-fold and 4.8-fold higher than that of HepG2 cells indicating that SNE is less cytotoxic to normal cells. Comparing to normal liver cells, SNE seems to have stronger death effect toward liver cancer cells, HepG2. We further determined the cytotoxicity of SNE on other normal cells, 3T3-L1 and cancer cells, MCF-7, MDA-MB-231 and AGS at various concentrations for 48 h followed by MTT assay. The results indicated that SNE is more cytotoxic to tumor cells.

SNE-Induced Apoptotic Death of HepG2 Cells. HepG2 cells treated with 2 and 5 mg/ml SNE for 48 h showed typical apoptotic features: cell shrinkage, membrane blebbing, and apoptotic bodies as observed under inverted microscopy. To further confirm the programmed cell death was involved in the cytotoxic effect of SNE on liver cancer cells, SNE-treated HepG2 cells were subjected to apoptosis assays by PI staining of nuclei as described in Materials and methods, and the apoptotic state was quantitated by flow cytometry. The results indicated that after atreatment with high concentration (2 and 5 mg/ml) of SNE for 48 h, an increased proportion of apoptotic cells were observed (Figure 3A). The ratio of cells at the hypodiploid phase were increased to 30.01% and 37.88% when HepG2 cells were exposed to 2.0 mg/ml and 5.0 mg/ml SNE for 48 h, respectively (Figure 3A). The results indicated that high doses of SNE induced apoptotic cell death in HepG2 cells.

Effect of SNE on JNK Phosphorylation and Bax Protein Expression. JNK plays an important role in apoptotic signaling. In some cell types, JNK regulate the activities of pre-existing Bcl-2 family proteins that mediate mitochondrial release of cytochrome *c*, resulting in caspase activation (*16*). We investigated whether the SNE-induced apoptosis was modulated by the activation of JNK. The results showed that the cellular level of phospho-JNK was significantly increased to 2.65-fold and 2.81-fold ($P < 0.001$) of control level under a treatment of 2 mg/ml and 5 mg/ml of SNE, respectively (Figure 3B). Investigations of the bcl-2 gene family that encodes integral membrane proteins have shown a complex network regulating apoptosis in multiple biological systems (*17*). We examined the cellular levels of Bax after the treatment of SNE for 48 h in HepG2 cells. The expressions of Bax were significantly induced by the treatment of 2 mg/ml and 5 mg/ml of SNE to 3.45-fold and 3.52-fold ($P < 0.001$), respectively (Figure 3B). SNE induced apoptotic cell death in HepG2 cells, as evidenced by increase in the expression of p-JNK and Bax.

Effect of SNL on Cytochrome *c* Release and Caspase 3 Cleavage. Since cytochrome *c* is reported to be involved in the activation of the caspase that executes apoptosis (*18*), we examined the level of cytochrome *c* in the cytosol by Western blot analysis. The results showed that the amount of cytosolic cytochrome *c* increased 1.88-fold and 2.05-fold ($P < 0.001$) in the 2 mg/ml and 5mg/ml SNE-treated HepG2 cells (Figure 3C). Caspases 3 is a cytosolic protein that exists normally as an inactive precursor with higher molecular weights (32 kDa) that is cleaved proteolytically into low molecular weights (20 kDa) when cell undergoes apoptosis (*19*). In this study, there was an increase in the activation of caspase 3 to 1.91-fold, 2.3-fold and 2.45-fold (**$P < 0.01$; ***$P < 0.001$) of control level in response to 1 mg/ml, 2 mg/ml and 5 mg/ml SNE treatment, respectively (Figure 3D). The results indicated that addition of SNE exerted an apoptotic effect in HepG2 cells by increases in the mitochondrial release of cytochrome *c* and activation of caspase 3.

Low Concentration of SNE-Induced Autophagic Cell Death in HepG2 Cells. The flow cytometric data (Figure 3A) showed that there was only a very small portion (< 4 %) of HepG2 cells displayed a typical morphology of apoptosis when the cells were exposed to low concentrations (50 to 1000 μg/ml) of SNE. At the same circumstances, the survival rates were down to 67.7% and 20% for 50 and 1000 μg/ml, respectively (Figure 2B). These observations indicated that some other death mechanism was initiated in HepG2 cells in response to the treatment of low concentrations (50 to 1000 μg/ml) of SNE.

Electron microscopic characterization, which has been the gold standard for determining the mode of cell death, was next used to distinguish between apoptosis, necrosis and nonapoptotic programmed cell death. Nonapoptotic programmed cell death is principally attributed to autophagy (type II programmed cell death). Autophagy is series of biochemical steps through which eukaryotic cells commit suicide by degrading their own cytoplasm and organelles through a process in which these components are engulfed and then digested in double membrane-bound vacuoles called autophagosomes (*20*). Transmission electron microscopic analysis of HepG2 cells without SNE treatment revealed normal nuclear and mitochondrial morphology (Figure4A-a). On the other hand, HepG2 cells treated with 100 μg/ml of SNE for 48 h revealed extensive vacuolization, formation of membranous whorls (also called myelin figures) and depletion of organelles, which are hallmarks of autophagy (Figure 4A-b,c). Cells undergoing autophagic cell death retained an intact nuclear membrane, without chromatin condensation. Initiation of autophagy was associated with an accumulation of lipid droplets in cytoplasm (fatty change of hepatocytes) (Figure 4A-b). This event is due to a decline in protein synthesis (vide infra) which blocks the utilization of lipids for lipid-protein conjugation and is typical of hepatocytes undergoing cellular stress (*21*).

Autophagy is characterized by AVO formation, which is detected and measured by vital staining of acridine orange. Acridine orange moves freely to cross biological membranes and accumulates in acidic compartment, where it is seen as fluorescence bright red (*22*). As shown in Figure 4B-b~f, vital staining of HepG2 cells with acridine orange showed the accumulation of AVO in the cytoplasm of cells exposed to 10~1000 μg/ml of SNE. In contrast, there were relatively few AVOs in the cytoplasm of control cells (Figure 4B-a). These data indicated that HepG2 cells treated with low concentration of SNE revealed morphology and ultrastructural changes of autophagocytic death and increased levels of autophagic vacuoles.

Involvement of LC3 in SNE-Induced Autophagy. LC3 is localized in autophagosome membranes during amino acid starvation-induced autophagy (*23*). Recent investigation showed that there are two forms of LC3 proteins in cells: LC3-I and LC3-II (*22*). LC3-I is the cytoplasmic form of LC3 and is processed into LC3-II, which is associated with the autophagosome membrane. Therefore, the amount of LC3-II is correlated with the extent of autophagosome formation. Using the immunoblotting analysis with anti-LC3 antibody, we examined the expressions of LC3-I (18 kDa) and LC3-II (16 kDa) in HepG2 cells treated with SNE. As shown in Figure 5A, the level of total LC3 (LC3-I and LC3-II proteins) increased in HepG2 cells 24 h after exposure to SNE. Moreover, a marked increase in LC3-II protein was also detected in these cells. These results indicate that SNE stimulated not only the accumulation of LC3 protein, but also the conversion of a fraction of LC3-I into LC3-II. LC3 was involved in the SNE-induced autophagy in HepG2 cells.

Effect of SNE on Bcl-2 Expression and Akt Phosphorylation. Autophagy is a multi-step process, and various signaling pathways have been implicated in its up- or down-regulation. Bcl-2 has also been shown to regulate autophagy in cancer cells. Down-regulation of Bcl-2 using antisense technology triggered autophagy, but not apoptosis, in HL60 human leukaemic cells (*24*). We investigated whether the SNE-induced autophagy was modulated by Bcl-2. The results showed that the cellular level of Bcl-2 was significantly decreased to 80%, 25% and 18% of that of control in the cells exposed to 100 μg/ml, 500 μg/ml and 1000 μg/ml of SNE treatment, respectively (Figure 5B). Furthermore, Akt is a serine-threonine kinase, located downstream of class I PI3K, that activates the kinase mTOR, leading to suppression of autophagy. We examined the level of phospho-Akt in the cytosol by Western blot analysis. The results showed that the amount of phospho-Akt decreased to 45%, 40% and 25% of control in the cells exposed to 100 μg/ml, 500 μg/ml and 1000 μg/ml of SNE treatment, respectively ($P < 0.001$) (Figure 5C). These results indicate that Bcl-2 and Akt were involved in the SNE-induced autophagy.

3-MA Partially Blocked the SNE-Induced LC3-II Conversion and Cell Death. To confirm the contribution of autophage in the SNE-induced cell death, we used the autophagy inhibitor 3-MA, a class III-PI3K inhibitor, to inhibit the autophagy. The MTT assays show that 2 mM 3-MA could partially prevent SNE-induced cell death (Figure 6B). The induction of LC3-I and LC3-II expression were also inhibited by 3-MA (Figure 6A). Based on these data, we concluded that SNE could induce HepG2 cells to undergo autophagic cell death.

DISCUSSION

Solanum nigrum L. (SN) is a common herb that grows wildly and abundantly in open field. It has been used in traditional folk medicine because of its diuretic and antipyretic effects. More specifically, it has been used to cure inflammation, edema, mastitis and hepatic cancer for a long time in oriental medicine (*25*). The phytochemical studies revealed the presence of an alkaloid called solamargine, nigrum I, nigrum II and a glycoside named solasodine (*7*). It has also been shown that SN contains many polyphenolic compounds, mainly flavonoids and steroids. Our results showed that SNE is consisting of 14.92% polysaccharides, 4.81% protein and 20.35% total polyphenols, such as gallic aicd (2.897%), PCA (1.977%), catechin (2.353%), caffeic acid (1.988%), epicatechin (0.392%), rutin (0.836%), naringenin (5.106%) and unknow polyphenols (Table 1, 2 and Figure 1). The antioxidant and anti-tumor activity of these extracts has been suggested to be due to the presence of polysaccharides and polyphenolic constituents. Nevertheless, there is little conclusive evidence demonstrating the effectiveness of SN on treating already existed 50 to 1000 μg/ml tumors or malignancies animals.

Our results demonstrated a significant cytotoxic effect of SNE on HepG2 cells that was mediated via two mechanisms depending on the exposed concentrations. When HepG2 cells were treated with high concentration (2 mg/ml and 5 mg/ml) of SNE, the cells underwent apoptotic cell death as evidenced by increases in sub-G1 cells, and cellular levels of phospho-JNK, Bax, cytosolic cytochrome *c* and cleaved-caspase 3. Exposure of low concentration (50~1000 μg/ml) of SNE did not result in apoptosis, but rather our results point to autophagocytosis (autophagy of type II programmed cell death) as the main mode of death under such condition.

Autophagy is a physiological mechanism that involves the sequestration of cytoplasm and intracellular organelles into membrane vacuoles and results in their eventual enzymatic degradation (*20*). In response to appropriate stimulation, depolarized mitochondria are known to move into autophagic vacuoles. Thus, mitochondrial dysfunction may be a point of overlap between apoptotic and autophagocytic processes (*26*). The fusion of the edges of the membrane sac forms a closed double-membrane structure, the so-called autophagosome. Finally, the autophagosome fuses with a lysosome to become the autolysosome within which lysosomal hydrolases degrade the sequestered cellular constituents. HepG2 cells treated with 50~1000 μg/ml of SNE demonstrated an ultrastructural appearance consistent with the characteristics of autophagy under electron microscopic observation.

Furthermore, SNE-treated cells were able to be stained with acridine orange, a specific marker for autophagic vacuoles (*22*). Confirmatory experiments were performed with anti-LC3 antibody showing that SNE stimulated not only the expression of LC3 protein, but also the conversion of a fraction of LC3-I into LC3-II. We also demonstrated that 3-MA could blocked the SNE-induced LC3-II conversion and cell death. Furthermore, the levels of Bcl-2 and Akt, that have been implicated in down-regulation of autophagy were decreased upon SNE treatment, confirming the involvement of Bcl-2 and Akt in the SNE-induced autophagy (*24*).

Nonapoptotic cell death is mainly attributed to autophagy that is considered to be an alternative way to kill tumor cells when the cells are chemoresistant on the basis of ineffective apoptosis. A number of studies have reported that autophagy is activated in cancer cells in response to various anticancer therapies, such as tamoxifen in breast cancer cells (*27*), temozolomide (TMZ, a DNA alkylating agent) and arsenic trioxide in malignant glioma cells (*28*). As for natural products, resveratrol, a phytoalexin that is present in grape nuts and red wine, induced autophagy in ovarian cancer cells (*29*), and soybeen B-group triterpenoid saponins caused autophagy in colon cancer cells (*30*). The results of present study add SNE to the list of natural products that possess autophagic effect in addition to its apoptotic effect. We have demonstrated that the cytotoxic effects after expose to high concentration (2 mg/ml and 5 mg/ml) SNE is caused by apoptosis and low concentration SNE is caused by autophagy. However, the molecular basis for the differentiate effect responding to high and low concentrations of SNE needs further investigation. There might be a cross-talk between the pathways of apoptosis and autophagy.

In summary, we have identified two distinct anti-neoplastic activities of SNE in liver cancer cells, the ability to induce apoptosis and autophagocytosis. This response and its ability to kill these cells hint at the possibility that this agent may be useful as an adjuvant therapy to treat liver tumors. These findings pave the way for additional experiments to consider the molecular basis for this response and studies to determine whether adequate concentrations of bioactive SNE can be attained to treat liver tumors.

Reference

(1) Tong, W. M.; Lee ,M. K.; Galendo, D.; Wang, Z. Q.; Sabapathy, K. Aflatoxin-B exposure does not lead to p53 mutations but results in enhanced liver cancer of Hupki (human p53 knock-in) mice. *Int. J. Cancer* **2006**, *119*, 745-749.

(2) Son, Y. O.; Kim, J.; Lim, J. C.; Chung, Y.; Chung, G. H.; Lee, J. C. Ripe fruit of Solanum nigrum L. inhibits cell growth and induces apoptosis in MCF-7 cells. *Food Chem. Toxicol.* **2003**, *41*, 1421-1428.

(3) Sultana, S.; Perwaiz, S.; Iqbal, M.; Athar, M. Crude extracts of hepatoprotective plants, Solanum nigrum and Cichorium intybus inhibit free radical-mediated DNA damage. *J. Ethnopharmacol.* **1995**, *45*, 189-192.

(4) Prashanth Kumar, V.; Shashidhara, S.; Kumar, M. M.; Sridhara, B. Y. Cytoprotective role of Solanum nigrum against gentamicin-induced kidney cell (Vero cells) damage in vitro. *Fitoterapia* **2001**, *72*, 481-486.

(5) Yen, G. C.; Chen, H. Y.; Peng, H. H. Evaluation of the cytotoxicity, mutagenicity and antimutagenicity of emerging edible plants. *Food Chem. Toxicol.* **2001**, *39*, 1045-1053.

(6) Lee, S. J.; Oh, P. S.; Ko, J. H.; Lim, K.; Lim, K. T. A 150-kDa glycoprotein isolated from Solanum nigrum L. has cytotoxic and apoptotic effects by inhibiting the effects of protein kinase C alpha, nuclear factor-kappa B and inducible nitric oxide in HCT-116 cells. *Cancer Chemother. Pharmacol.* **2004**, *54*, 562-572.

(7) Raju, K.; Anbuganapathi, G.; Gokulakrishnan, V.; Rajkapoor, B.; Jayakar, B.; Manian, S. Effect of dried fruits of Solanum nigrum LINN against CCl_4-induced hepatic damage in rats. *Biol. Pharm. Bull.* **2003**, *26*, 1618-1619.

(8) Ikeda, T.; Tsumagari, H.; Nohara, T. Steroidal oligoglycosides from Solanum nigrum. *Chem. Pharm. Bull. (Tokyo)* **2000**, *48*, 1062-1064.

(9) Lakenbrink, C.; Lapczynski, S.; Maiwald, B.; Engelhardt, U. H. Flavonoids and other polyphenols in consumer brews of tea and other caffeinated beverages. *J. Agric. Food Chem.* **2000**, *48*, 2848-2852.

(10) La Torre, G. L.; Saitta, M.; Vilasi, F.; Pellicano`, T.; Dugo, G. Direct determination of phenolic compounds in Sicilian wines by liquid chromatography with PDA and MS detection. *Food Chemistry*.**2006**, *94*, 640-650.

(11) Mosmann, T. Rapid colorimetric assay for cellular growth and survival: application to proliferation and cytotoxicity assays. *J. Immunol. Methods* **1983**, *65*, 55-63.

(12) Sherwood, S. W.; Schimke, R. T. Cell cycle analysis of apoptosis using flow cytometry. *Methods Cell Biol.* **1995**, *46*, 77-97.

(13) Jiang, S. T.; Liao, K. K.; Liao, M. C.; Tang, M. J. Age effect of type I collagen on morphogenesis of Mardin-Darby canine kidney cells. *Kidney Int.* **2000**, *57*, 1539-1548.

(14) Kanzawa, T.; Kondo, Y.; Ito, H.; Kondo, S.; Germano, I. Induction of autophagic cell death in malignant glioma cells by arsenic trioxide. *Cancer Res.* **2003**, *63*, 2103-2108. (15) Gutierrez-Ruiz, M. C.; Bucio, L.; Souza, V.; Gomez, J. J.; Campos, C.; Carabez, A. Expression of some hepatocyte-like functional properties of WRL-68 cells in culture. *In Vitro Cell Dev. Biol. Anim.* **1994**, *30*, 366-371.

(16) Tournier, C.; Hess, P.; Yang, D. D.; Xu, J.; Turner, T. K.; Nimnual, A.; Bar-Sagi, D.; Jones, S. N.; Flavell, R. A.; Davis, R. J. Requirement of JNK for stress-induced activation of the cytochrome *c*-mediated death pathway. *Science* **2000**, *288*, 870-874.

(17) Danial, N. N.; Korsmeyer, S. J. Cell death: critical control points. *Cell* **2004**, *116*, 205-219.

(18) Yang, J.; Liu, X.; Bhalla, K.; Kim, C. N.; Ibrado, A. M.; Cai, J.; Peng, T. I.; Jones, D. P.; Wang, X. Prevention of apoptosis by Bcl-2: release of cytochrome c from mitochondria blocked. *Science* **1997**, *275*, 1129-1132.

(19) Solary, E.; Plenchette, S.; Sordet, O.; Rebe, C.; Ducoroy, P.; Filomenko, R.; Bruey, J. M.; Droin, N.; Corcos, L. Modulation of apoptotic pathways triggered by cytotoxic agents. *Therapie* **2001**, *56*, 511-518.

(20) Reggiori, F.; Klionsky, D. J. Autophagy in the eukaryotic cell. *Eukaryot. Cell* **2002**, *1*, 11-21.

(21) Martinet, W.; DeMeyer, G. R.; Andries, L.; Herman, A. G.; Kockx, M. M. In situ detection of starvation-induced autophagy. *J. Histochem. Cytochem.* **2006**, *54*, 85-96.

(22) Stankiewicz, M.; Jonas, W.; Hadas, E.; Cabaj, W.; Douch, P. G. Supravital staining of eosinophils. *Int. J. Parasitol.* **1996**, *26*, 445-446.

(23) Mizushima, N.; Yamamoto, A.; Hatano, M.; Kobayashi, Y.; Kabeya, Y.; Suzuki, K.; Tokuhisa, T.; Ohsumi, Y.; Yoshimori, T. Dissection of autophagosome formation using Apg5-deficient mouse embryonic stem cells. *J. Cell Biol.* **2001**, *152,* 657-668.

(24) Kondo, Y.; Kanzawa, T.; Sawaya, R.; Kondo, S. The role of autophagy in cancer development and response to therapy. *Nat. Rev. Cancer* **2005**, *5*, 726-734.

(25) Heo, K. S.; Lee, S. J.; Ko, J. H.; Lim, K.; Lim, K. T. Glycoprotein isolated from Solanum nigrum L. inhibits the DNA-binding activities of NF-kappaB and AP-1, and increases the production of nitric oxide in TPA-stimulated MCF-7 cells. *Toxicol. In Vitro,* **2004**, *18*, 755-763.

(26) Ogier-Denis, E.; Codogno, P. Autophagy: a barrier or an adaptive response to cancer. *Biochim, Biophys, Acta.* **2003**, *1603*, 113-128.

(27) Scarlatti, F.; Bauvy, C.; Ventruti, A.; Sala, G.; Cluzeaud, F.; Vandewalle, A.; Ghidoni, R.; Codogno, P. Ceramide-mediated macroautophagy involves inhibition of protein kinase B and up-regulation of beclin 1. *J. Biol. Chem.* **2004**, *279*, 18384-18391.

(28) Kanzawa, T.; Germano, I. M.; Komata, T.; Ito, H.; Kondo, Y.; Kondo, S. Role of autophagy in temozolomide-induced cytotoxicity for malignant glioma cells. *Cell Death Differ*. **2004**, *11*, 448-457.

(29) Opipari, A. W.Jr.; Tan, L.; Boitano, A. E.; Sorenson, D. R.; Aurora, A.; Liu, J. R. Resveratrol-induced autophagocytosis in ovarian cancer cells. *Cancer Res.* **2004**, *64*, 696-703.

(30) Ellington, A. A.; Berhow, M. A.; Singletary, K. W. Inhibition of Akt signaling and enhanced ERK1/2 activity are involved in induction of macroautophagy by triterpenoid B-group soyasaponins in colon cancer cells. *Carcinogenesis* **2006**, *27*, 298-306.

成果自評：(1) 提出龍葵為新的anticancer agents。

(2) 說明抗癌的機轉。

(3) 提供食物成份在抗癌研究的模式。

圖表

Table 1. The dry weight, polyphenol, polysaccharide and protein content of water extract of *Solanum Nigrum* L. (SNE).

SNE	%
Dry weight	23.13 ± 2.095
Polyphenol	20.35 ± 0.967
Polysaccharide	14.92 ± 1.333
Protein	4.81 ± 0.422

Table 2. Characterization of phenolic compounds of SNE

Peak No.	Retention time (min)	Assigned identity	Recovery %	UV λ_{max} (nm)	$[M-H]^-$ *m/z*	LC/ESI-MS[2]* *m/z*
1	6.20	Gallic acid	2.897 ± 1.1	270, 225	168.9	125.0
2	13.49	PCA	1.977 ± 0.95	222, 259	153.1	108.9
3	31.48	Catechin	2.353 ± 1.05	230, 229	289.1	245.2, 205.1
4	32.84	Caffeic acid	1.533 ± 0.63	256, 354	178.9	135.0
5	35.61	Epicatechin	1.988 ± 0.49	230, 279	289.0	245.1
6	40.35	Rutin	0.836 ± 0.32	256, 354	609.2	301.1, 343.1
7	49.16	Narigenin	5.106 ± 2.01	231, 288	271.1	150.9, 177.1

*MS[2] run with 30% collision energy.

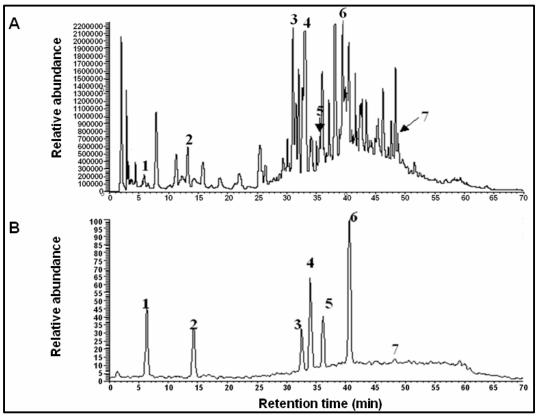

Figure 1. (A) HPLC/UV chromatogram (278 nm) of the water extract of *Solanum Nigrum* L. (SNE). Polyphenolic compounds correspond to peaks 1-7 in (B) were marked.

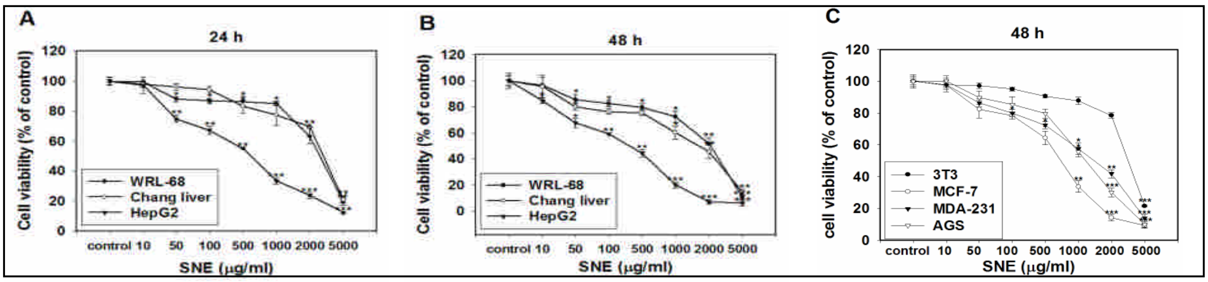

Figure 2. Effects of SNE on the viability of tumor cells (HepG2, Chang liver, MCF-7, MDA-231, and AGS cells) and normal cells (WRL-68 and 3T3 cells).

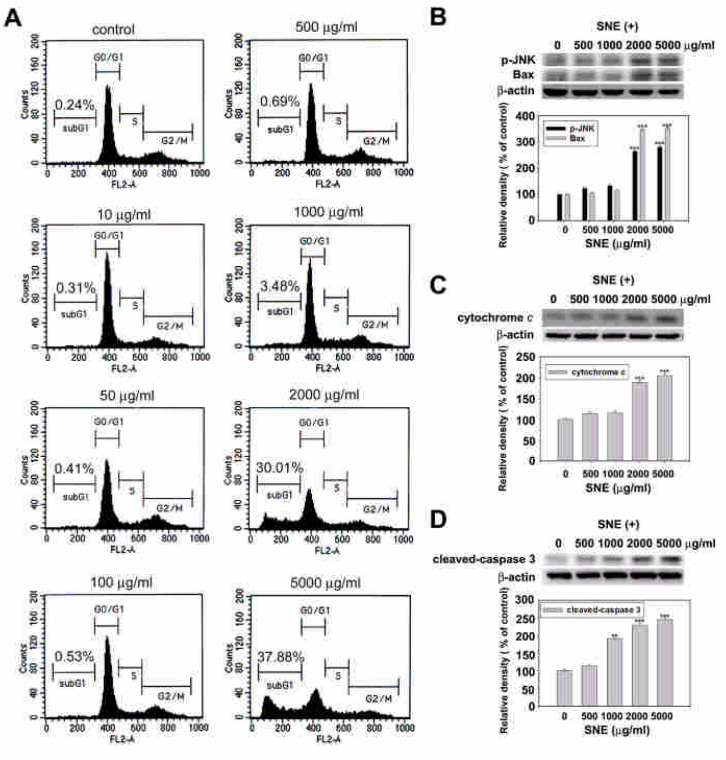

Figure 3. Apoptosis effects of SNE on HepG2

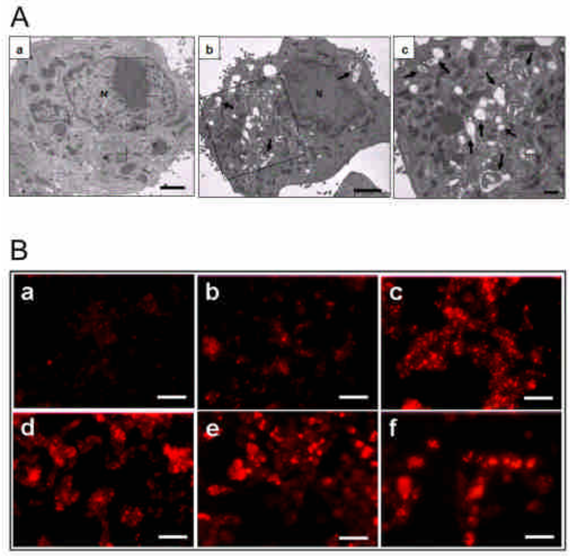

Figure 4. SNE-induced autophagic death in HepG2 cells.

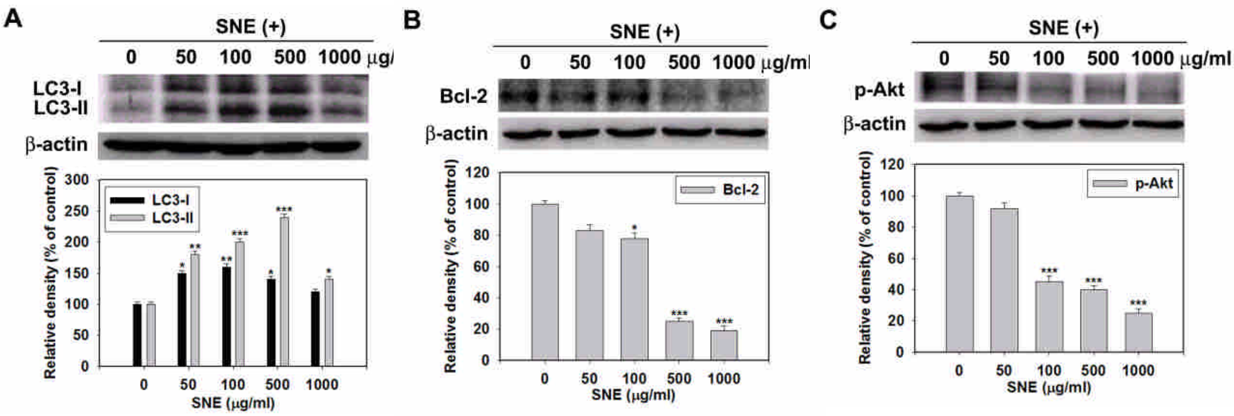

Figure 5. Involvement of LC3, Bcl-2 and p-Akt in SNE-induced autophagy in HepG2 cells.

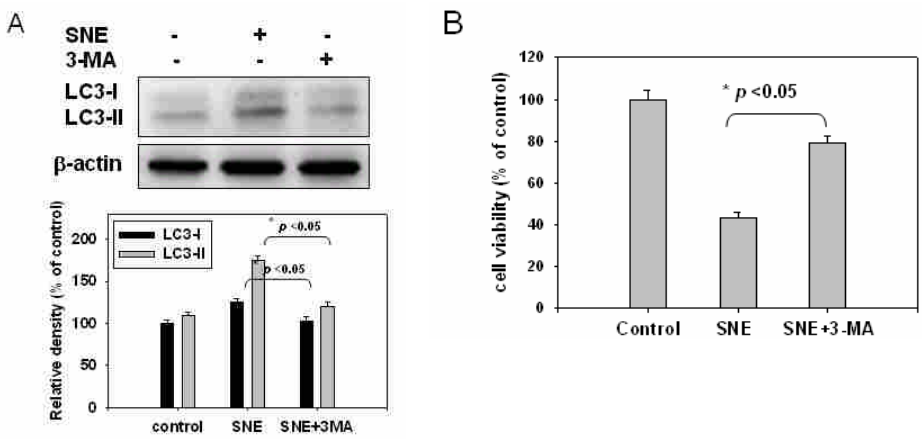

Figure 6. 3-MA partially blocked the SNE-induced LC3 expression and cell death.